2011 International Symposium on Nonlinear Theory and its Applications
NOLTA2011, Kobe, Japan, September 4-7, 2011

Chaotic Gas Turbine Simulating the Motion of Convective Heat Flow

Kenichiro Cho, Yuki Okada, Jungo Tatsutani, Toshiyuki Toriyama and Takaya Miyano

Department of Micro System Technology, Ritsumeikan University
1-1-1 Noji-Higashi, Kusatsu, Shiga, 525-8577 Japan
Email: tmiyano@se.ritsumei.ac.jp

Abstract—Being inspired by the chaotic waterwheel whose rotational motion is governed by the Lorenz equations, invented by Malkus and Howard in 1970s, we have developed a chaotic gas turbine that simulates the dynamical behavior of the Rayleigh-Bénard convection heated from below. We show the equations of motion of our gas turbine and compare numerical solutions with experimental observations for the angular velocity of the rotor. The relationship between the Lorenz equations and our equations is discussed.

1. Introduction

The chaotic waterwheel, invented by Malkus and Howard in 1970s [1, 2], displays random reversals of rotational motion that are governed by the Lorenz equations [3, 4]. The chaotic motion is a realization of the Lorenz attractor often referred to as the double scroll. The Lorenz equations, which were derived using mode truncation from the Boussinesq-Oberbeck equations, are an oversimplified physical model for the Rayleigh-Bénard convection heated from below. In the chaotic waterwheel, the three physical forces that drive thermal convective flows, i.e., buoyancy, frictional force and thermal dissipation, are simulated by the gravity of water, the frictional force on the axis of the waterwheel and the leakage of water from the vessels of the waterwheel, respectively. In this context, the waterwheel is subject to the physics of thermal convection.

Being inspired by the chaotic waterwheel, we have developed a chaotic gas turbine that displays random reversals of rotational motion. Although the three physical forces driving thermal convection are simulated as well in our gas turbine in a similar manner to the chaotic waterwheel to model the dynamical behavior of convective heat flows, the rotational motion of our gas turbine appears to be more complex than that of the chaotic waterwheel. As will be shown in this paper, it turns out that our machine obeys different equations of motion from those of the chaotic waterwheel and the nondimensionalized expression of our equations may be referred to as augmented Lorenz equations. In this paper, we show the equations of motion of our gas turbine, assess their performance through the comparison of numerical solutions with experimentally observed angular velocity of the turbine as a function time and discuss the relationship between the Lorenz equations and our equations.

2. Chaotic Gas Turbine and its Equations of Motion

In this section, we give a brief description about our gas turbine. Details will be shown [5]. Figure 1 shows a photograph of the rotor of our gas turbine. The whole structure of the turbine can be seen on the video in [4]. The schematic of the rotor is depicted in Fig. 2. Our gas turbine is of planar type that is often used for gas turbine engines as micro-electro-mechanical power systems [6, 7]. The turbine has a stainless steel rotor sandwiched in three layers of acrylic plates. The diameter of the rotor is 40 [mm]. Thin flat turbine blades are settled on the rotor with radial symmetry. As shown in Fig. 2, the air inflow impinges the turbine blades near the inlet within $\pm\phi$ about the central horizontal axis of the turbine. This simulates buoyancy in thermal convection. Part of the air leaks out of the turbine through the narrow channels on the rotor, which simulates thermal dissipation in thermal convection. The frictional force is generated by a hydrostatic thrust bearing.

Under the assumptions of infinitely many turbine blades with a negligible thickness, the working fluid as an ideal gas and the driving force due to air inflow pressure concentrating at the center of mass of the blade located at the distance r from the center of the rotor, the equations of motion can be expressed as the following system of ordinary differential equations.

$$\dot{\mathbf{a}} = \omega \mathbf{n}\mathbf{b} - (K+\alpha)\mathbf{a} \ , \tag{1}$$

$$\dot{\mathbf{b}} = -\omega \mathbf{n}\mathbf{a} - (K+\alpha)\mathbf{b} + \frac{2\alpha P_{in}}{\pi}\mathbf{n}^{-1}\mathbf{W} \ , \tag{2}$$

$$\dot{\omega} = -\frac{v\omega}{I} + \frac{Sr}{I}\mathrm{tr}(\mathbf{\Phi a}) \ , \tag{3}$$

where ω denotes the angular velocity of the rotor whose inertial moment is approximately $I = 1.5 \times 10^{-5}$ [kgm^2], α and K are constants associated with

the air inflow and the air leakage, respectively, P_{in} is the air inflow pressure, v is the damping rate of friction, S is the area of the blade, and tr$(\cdot)$ represents the diagonal sum of a matrix. Here, the diagonal components of $N \times N$ square diagonal matrices with $N \to \infty$,

$$\mathbf{a} = \begin{pmatrix} a_1 & 0 & \cdots & 0 \\ 0 & a_2 & \ddots & \vdots \\ \vdots & \ddots & \ddots & 0 \\ 0 & \cdots & 0 & a_N \end{pmatrix}$$

and

$$\mathbf{b} = \begin{pmatrix} b_1 & 0 & \cdots & 0 \\ 0 & b_2 & \ddots & \vdots \\ \vdots & \ddots & \ddots & 0 \\ 0 & \cdots & 0 & b_N \end{pmatrix}$$

represent the sinusoidal and cosinusoidal Fourier coefficients of the air inflow pressure, respectively. In the Fourier expansion of the inflow pressure, the following diagonal matrices are defined:

$$\mathbf{n} = \begin{pmatrix} 1 & 0 & \cdots & 0 \\ 0 & 2 & \ddots & \vdots \\ \vdots & \ddots & \ddots & 0 \\ 0 & \cdots & 0 & N \end{pmatrix} ,$$

$$\mathbf{W} = \begin{pmatrix} \sin\phi & 0 & \cdots & 0 \\ 0 & \sin 2\phi & \ddots & \vdots \\ \vdots & \ddots & \ddots & 0 \\ 0 & \cdots & 0 & \sin N\phi \end{pmatrix}$$

and $\mathbf{\Phi} = \mathrm{diag}\Big(\phi - \frac{1}{2}\sin 2\phi \ \cdots \ \frac{1}{n-1}\sin(n-1)\phi - \frac{1}{n+1}\sin(n+1)\phi \ \cdots \ \frac{1}{N-1}\sin(N-1)\phi - \frac{1}{N+1}\sin(N+1)\phi\Big)$. It turns out that our equations of motion are equivalent to an augmented version of the Lorenz equations, as will be show in the next section.

3. Results and Discussion

To verify the validity of Eqs.(1)–(3), we manufactured the turbine, observed the angular velocity of the rotor as a function of time and compared numerical solutions of the equations with the experimental data. The turbine has 24 blades and the adjacent angle between blades is approximately $\pi/12 \approx 0.26$ [rad]. To measure the angular velocity $\omega(t)$, a couple of photoelectric sensors were placed above the turbine at two locations off-symmetrical with respect to the central horizontal axis of the turbine. The sensor systems recorded the times at which two turbine blades crossed the two light beams (the two red spots on the rotor in the video shown in [4]) that emanated from the sensor systems. The difference in reflectance between the blade surface and the rotor body allows the sensor systems to detect the blades crossing the light spots. The off-symmetrical setting of the sensors enables us to detect changes in the direction of rotation. With the adjacent angle between blades and the time for the blades to cross either of the light spots, the angular velocity of the rotor, as well as its sense of rotation, can be estimated as a function of time, although the data points on the time series are not equidistant in time.

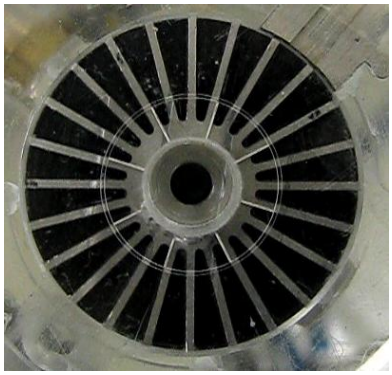

Figure 1: Actual chaotic gas turbine.

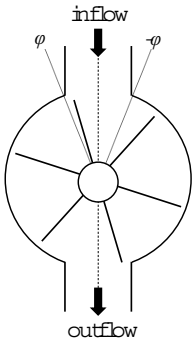

Figure 2: Schematic of chaotic gas turbine.

Figure 3 shows a time series of $\omega(t)$ observed for the turbine operated under 20.5 [kPa] of the air inflow pressure (gauge pressure) and 5.3 [kPa] of the thrust bearing pressure (589 data points). To obtain the corresponding numerical data, we ran Eqs. (1)–(3) using the fourth-order Runge-Kutta method with a time width of 0.002 [sec] under the parameter settings of

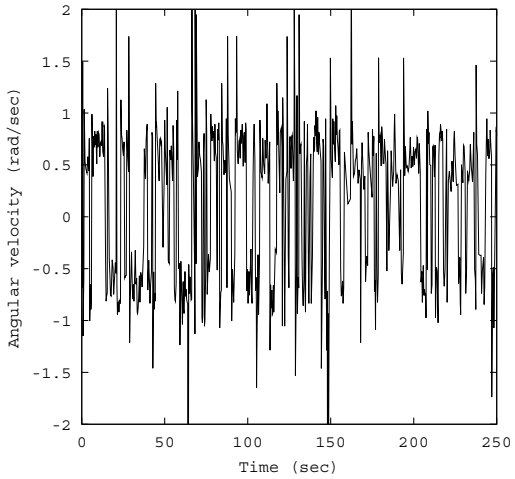

Figure 3: Actually observed angular velocity as a function of time (589 data points). The data points are not equidistant in time. $P_{in} = 20.5$ [kPa] and thrust bearing pressure = 5.3 [kPa] (gauge pressure).

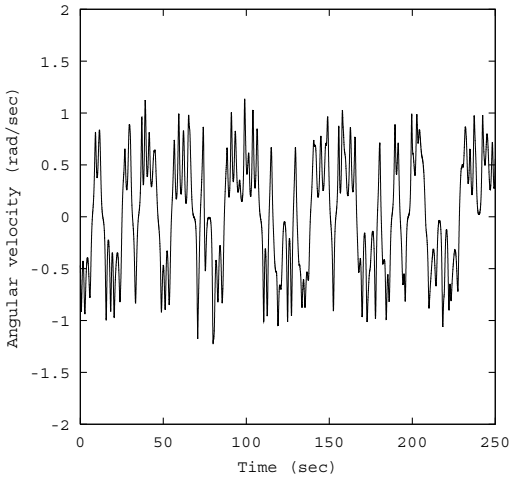

Figure 4: Numerically calculated angular velocity as a function of time (125 000 data points). $N = 1000$. The data points are equidistant in time. $P_{in} = 20.5$ [kPa].

$P_{in} = 20.5$ [kPa], $N = 1000$, $v = 1.7 \times 10^{-5}$ [kgm/sec], $\phi = 0.36$ [rad], $S = 2 \times 10^{-5}$ [m^2], $r = 0.015$ [m], $K = 0.01$ [sec^{-1}] and $\alpha = 0.03$ [sec^{-1}]. Initial 125 000 data points were discarded to eliminate the transient part that is dependent on the initial conditions $\omega(0) = 0$ and $a_n(0)$ and $b_n(0)$ as Gaussian random numbers with mean 0 and variance 1. Figure 4 shows numerical solutions $\omega(t)$ (125 000 data points). Despite noise contamination and nonequidistant sampling in time of the experimental data, Fig. 4 seems to capture the overall feature of the corresponding actual data.

Figure 5 shows the power spectra of numerical $\omega(t)$ estimated from 65536 data points. The power spectra have a broadband structure with no sharp peaks. Hence, the rotational motion of the turbine can be considered chaotic.

To make clear the relationship between our equations of motion and the Lorenz equations, we nondimensionalize Eqs. (1)–(3) using the following equations. Details will be shown in [5].

$$\mathbf{a} = \delta\mathbf{Y} \ , \tag{4}$$

$$\mathbf{b} = \beta\mathbf{Z} + \frac{2\alpha P_{in}}{(K+\alpha)\pi}\mathbf{n}^{-1}\mathbf{W} \ , \tag{5}$$

$$\omega = \mathrm{tr}(\gamma\mathbf{X}) \ , \tag{6}$$

$$t = T\tau \ ,$$

where $\mathbf{X}$, $\mathbf{Y}$ and $\mathbf{Z}$ are dimensionless $N \times N$ matrices with $N \to \infty$, β, δ and γ are square coefficient matrices, and τ and T are a dimensionless time and a coefficient, respectively. Introducing a scalar variable $X = \mathrm{tr}((\mathbf{n}^{-1})^2\mathbf{X})$, we obtain a dimensionless expression of the equations of motion as

$$\frac{dX}{d\tau} = \sigma\left[\mathrm{tr}\left((\mathbf{n}^{-1})^2\mathbf{Y}\right) - X\right] \ , \tag{7}$$

$$\frac{d\mathbf{Y}}{d\tau} = \mathbf{R}X - \mathbf{n}\mathbf{Z}X - \mathbf{Y} \ , \tag{8}$$

$$\frac{d\mathbf{Z}}{d\tau} = \mathbf{n}\mathbf{Y}X - \mathbf{Z} \ , \tag{9}$$

$$\sigma = \frac{v}{I(K+\alpha)} \ , \tag{10}$$

$$\mathbf{R} = \frac{2\alpha S r P_{in}}{(K+\alpha)^2 v\pi}\mathbf{n}^2\mathbf{\Phi}\mathbf{W} \ . \tag{11}$$

When $N = 1$, the nodimensionalized equations are exactly equivalent to the Lorenz equations with an aspect ratio of unity. Hence, the nodimensionalized equations of motion can be said to be an augmented version of the Lorenz equations, which are different from the previous extensions of the Lorenz equations studied in [8, 9]. We may call our nondimesionalized equations as augmented Lorenz equations. The augmented Lorenz equations can be viewed as a network of N Lorenz subsystems with scaled Rayleigh numbers defined by Eq. (11). This suggests that the augmented Lorenz equations may inherit the dynamical nature of the Lorenz equations such as synchronizability between augmented Lorenz oscillators [10].

4. Conclusions

We have developed the chaotic gas turbine subject to the augmented Lorenz equations. The augmented Lorenz equations can be viewed as a network of N Lorenz subsystems with $N \to \infty$ sharing the nondimensionalized angular velocity X as the central node. The overall feature of the temporal fluctuations

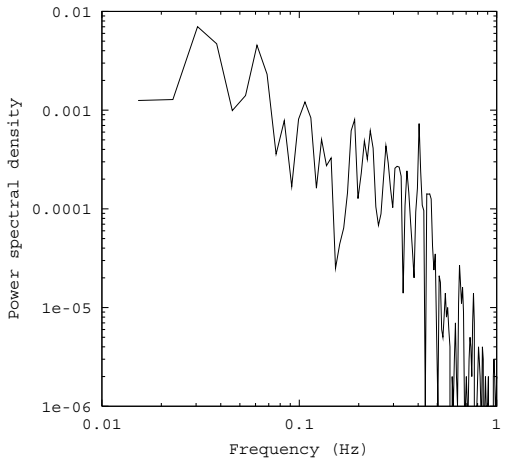

Figure 5: Power spectra of numerical angular velocity ($N = 1000$). 65536 data points are used for spectral estimation. $P_{in} = 20.5$ [kPa].

in the angular velocity might be reminiscent of the mean wind reversals observed for actual turbulent heat flows at high Rayleigh numbers [11]–[14]. The dynamical properties of the augmented Lorenz equations and their applications are open questions to be solved in our future studies.

Acknowledgments

We would like to thank Dr. Hiroshi Gotoda for stimulating discussion. This study was supported by JSPS Grant-in-Aid for Scientific Research (C) No. 22500214.

References

[1] S. H. Strogatz, *Nonlinear Dynamics and Chaos* (Addison-Wesley, Massachusetts, 1994) Chapter 9.

[2] M. Kolar and G. Gumbs, "Theory for the experimental observation of chaos in a rotating waterwheel," *Phys. Rev.* A, vol.45, pp.626–637, 1992.

[3] E. N. Lorenz, "Deterministic non-periodic flow," *J. Atoms. Sci.*, vol.20, pp.130–141, 1963.

[4] A video of a chaotic waterwheel manufactured by the authors on the basis of the mechanical design shown in [1] can be seen at the following URL: //www.ritsumei.ac.jp/se/ ~tmiyano/waterwheel09.html. A video of our gas turbine can also be seen at this URL.

[5] K. Cho, T. Miyano, A. Farhdhyan, Y. Okada and T. Toriyama, "Chaotic gas turbine subject to augmented Lorenz equations," unpublished.

[6] A. H. Epstein and S. D. Senturia, "Macro Power from Micro Machinery," *Science*, vol.276, p.1211, 1997.

[7] A. H. Epstein, "Millimeter-scale, Micro-Electro-Mechanical Systems Gas Turbine Engines," *ASME J. Eng. Gas Turbine Power*, vol.126, pp.205–226, 2004.

[8] Curry, J. H. A Generalized Lorenz System. *Commun. Math. Phys.*, vol.60, pp.193–204, 1978.

[9] McLaughlin, J. B. & Martin, P. C. Transition to turbulence in a statically stressed fluid system. *Phys. Rev.* A, vol.12, pp.186–203, 1975.

[10] K. Cho, J. Tatsutani and T. Miyano, "Chaotic Synchronization of Augmented Lorenz Systems," to appear in *Proc. 2011 Int. Symp. Nonlinear Theory and Its Applications*.

[11] Kadanoff, L. P. Turbulent heat flow: Structures and scaling. *Phys. Today*, vol.54, no.8, pp.34–39, 2001.

[12] K. R. Sreenivasan, A. Bershadskii and J. J. Niemela, "Mean wind and its reversal in thermal convection," *Phys. Rev.* E, vol.65, 056306-1–056306-11, 2002.

[13] A. Bershadskii, "Chaos from turbulence: Stochastic-chaotic equilibrium in turbulent convection at high Rayleigh numbers," *Chaos*, vol.20, 043124-1–043124-5, 2010.

[14] T. Yanagisawa, Y. Yamagishi, Y. Hamano,Y. Tasaka and Y. Takeda, "Spontaneous flow reversals in Rayleigh-Bénard convection of a liquid metal," *Phys. Rev.* E, vol.83, pp.036307-1–036307-6, 2011.